JOURNAL OF GEOPHYSICAL RESEARCH, VOL. 115, D06108, doi:10.1029/2009JD012742, 2010



# Associations between stratospheric variability and tropospheric blocking

T. Woollings,[1] A. Charlton-Perez,[1] S. Ineson,[2] A. G. Marshall,[3] and G. Masato[1]

Received 26 June 2009; revised 15 September 2009; accepted 5 November 2009; published 27 March 2010.

[1] There is widely believed to be a link between stratospheric flow variability and stationary, persistent "blocking" weather systems, but the precise nature of this link has proved elusive. Using data from the ERA-40 Reanalysis and an atmospheric general circulation model (GCM) with a well-resolved stratosphere (HadGAM), it is shown that there are in fact several different highly significant associations, with blocking in different regions being related to different patterns of stratospheric variability. This is true in both hemispheres and in both data sets. The associations in HadGAM are shown to be very similar to those in ERA-40, although the model has a tendency to underestimate both European blocking and the wave number 2 stratospheric variability to which this is related. Although the focus is on stratospheric variability in general, several of the blocking links are seen to occur in association with the major stratospheric sudden warmings. In general, the direction of influence appears to be upward, as blocking anomalies are shown to modify the planetary stationary waves, leading to an upward propagation of wave activity into the stratosphere. However, significant correlations are also apparent with the zonal mean flow in the stratosphere leading the occurrence of blocking at high latitudes. Finally, the underestimation of blocking is an enduring problem in GCMs, and an example has recently been given in which improving the resolution of the stratosphere improved the representation of blocking. Here, however, another example is given, in which increasing the stratospheric resolution unfortunately does not lead to an improvement in blocking.

**Citation:** Woollings, T., A. Charlton-Perez, S. Ineson, A. G. Marshall, and G. Masato (2010), Associations between stratospheric variability and tropospheric blocking, *J. Geophys. Res.*, *115*, D06108, doi:10.1029/2009JD012742.

## 1. Introduction

[2] It is widely believed that stratospheric sudden warmings are often accompanied by blocking weather patterns in the troposphere [e.g., *Andrews et al.*, 1987]. Detailed examples of such cases have been described in the literature, for example by *Labitzke* [1965], *O'Neill et al.* [1994], *Kodera and Chiba* [1995], and *Nishii et al.* [2009], and a systematic study of several events was performed by *Quiroz* [1986], who identified a stratosphere-blocking link in 85% of cases. Recently the issue was revisited in a longer data set by *Taguchi* [2008] who in contrast did not find any significant changes in blocking activity either in the periods before or after sudden warmings. *Martius et al.* [2009], however, do find a significant link between the two.

[3] The stratosphere-blocking link is of interest for two practical reasons. Firstly, the recent evidence of downward propagation of annular mode anomalies from the stratosphere to the troposphere [*Baldwin and Dunkerton*, 2001] has motivated a deeper understanding of how and why sudden warmings occur, so investigation into the dynamical mechanisms by which blocking could perturb the stratosphere is needed. *Polvani and Waugh* [2004] demonstrated that enhanced tropospheric wave activity precedes changes in the stratospheric annular mode, and it is likely that blocking contributes to this tropospheric wave activity. Secondly, blocking is itself a dramatic regional weather event, which can result in persistent anomalous weather conditions, and yet its simulation in weather and climate models is often regrettably poor [*D'Andrea et al.*, 1998]. If there is some way in which the stratosphere influences blocking, even if only through the passive removal of wave activity from the troposphere, then numerical models may need to have an accurate representation of the stratosphere if their simulation of blocking is to improve.

[4] There are several reasons why the precise nature of the stratosphere-blocking link may be difficult to pin down. Blocking can occur at many different locations, and often does so several times within a season, so establishing which blocking regions are linked to sudden warmings, and with what time lag, is difficult. This situation is compounded by the rarity of sudden warmings, resulting in small sample

[1]Department of Meteorology, University of Reading, Reading, UK.
[2]Hadley Centre, Met Office, Exeter, UK.
[3]Centre for Australian Weather and Climate Research, Hobart, Tasmania, Australia.


0148-0227/10/2009JD012742

sizes for statistical analyses. Furthermore there is no unique, widely accepted criteria to identify blocking. There are several different blocking indices in the literature and results from these can differ, even with respect to which are the dominant climatological regions of blocking. There are two general approaches to defining a blocking event, either as a reversed meridional gradient in a quantity such as geopotential height (as in the popular *Tibaldi and Molteni* [1990] index), or simply as a large and persistent anticyclonic anomaly, as in the work of *Dole and Gordon* [1983]. The index used here, as described in section 2.3, follows the former approach and emphasizes the stationary and persistent nature of blocking, as well as the dynamical wave breaking responsible for it. See *Tyrlis and Hoskins* [2008] for a more detailed discussion.

[5] Here we adopt a new approach in an attempt to circumvent some of these problems. Rather than focus on the small number of sudden warming events, we search for links between blocking and stratospheric variability in general, which then allows us the use of the whole reanalysis data set. We use a two-dimensional blocking index which searches for blocking events at all latitudes and longitudes, in contrast to many indices which only search along certain latitudes. In this way we can identify specific regions in which blocking is linked to stratospheric variability, although rigorous statistical tests for field significance will need to be applied. In addition we also supplement the observational record with the output from a simulation of a stratosphere-resolving numerical climate model. It will be seen that there are not one, but several different stratosphere-blocking links, all of which are of high statistical significance and are reproduced very well in the model data set. In fact, the existence of several different links may be a key reason for the contradictory results of different studies.

[6] After description of the data and methods used in section 2, the results of the correlation analysis will be presented in section 3. In section 4 we then examine some of the regions where blocking has a particularly strong link to stratospheric variability and investigate the evolution of events in these regions, in the hope that this will suggest physical mechanisms behind the observed correlations. While the inclusion of all stratospheric variability identifies relations with very high statistical significance, it is of interest whether some of these relations are evident in the sudden warming events, and this is investigated in section 5. The recent northern winter of 2008–2009 exhibited a dramatic sudden warming and tropospheric blocking, so we also analyze this winter (which is outside of the period of the reanalysis data used) to see if the events of this winter are consistent with the observed stratosphere-blocking links. We finish in section 6 with a brief analysis of two parallel model runs, one with a well resolved stratosphere and one without, to determine if the occurrence of blocking in the model is increased when the stratosphere is resolved.

## 2. Data and Methods

### 2.1. Data

[7] The majority of this paper uses 1.125° data from the European Centre for Medium-range Weather Forecasting reanalysis ERA-40 [*Uppala et al.*, 2005]. We focus on the two "active seasons" for stratosphere-troposphere interaction, namely November–March (NDJFM) in the Northern Hemisphere and August–November (ASON) in the Southern Hemisphere [*Thompson and Wallace*, 2000; *Baldwin et al.*, 2003; *Black and McDaniel*, 2007]. Altogether there are 44 complete northern seasons (1957/58–2000/01) and also 44 complete southern seasons (1958–2001). The results are not sensitive to inclusion of data from the presatellite period, as discussed in section 3.

[8] We compare the ERA-40 data with output from the Met Office Hadley Centre atmospheric general circulation model HadGAM1 [*Martin et al.*, 2006]. The model resolution is 1.875° longitude by 1.25° latitude and is used here in an extended vertical configuration with 60 levels and the upper boundary at 84 km to improve the representation of the stratosphere. The model is forced with observed SSTs and sea ice [*Rayner et al.*, 2003] and radiative forcings for the period 1961–2002, so providing 42 complete seasons in both hemispheres. Blocking in the 38 level climate resolution version of this model is described by *Ringer et al.* [2006] and sensitivity of Pacific blocking to tropical SST is explored by *Hinton et al.* [2009].

[9] In section 6 we compare the blocking climatology in 38 and 60 level configurations of HadGAM1. Note that this is a slightly different model to that used for the correlation analysis, for which a parallel L38 simulation was not available. This model includes many of the changes proposed for HadGEM2-A as documented by *Collins et al.* [2008]. The 38 level version (L38) has a model top in the stratosphere at 39.3 km (~3 hPa) and the 60 level version (L60) has a model top near the mesopause at 84.1 km (~0.004 hPa). Both models have the same vertical resolution in the troposphere with 28 identical levels below the tropopause, but different vertical resolutions in the stratosphere; the L38 (L60) model has 8 (13) levels in the middle and lower stratosphere between 10 and 100 hPa, and 2 (19) levels above 10 hPa. Importantly, both models also have the same gravity wave drag parameters, horizontal resolution and a timestep of 20 min, allowing for a clean assessment of the impact of stratospheric resolution. We produce 5 month model hindcasts for a suite of 15 winters over the last 45 years; 1962–1963, 1963–1964, 1964–1965, 1968–1969, 1974–1975, 1982–1983, 1983–1984, 1987–1988, 1989–1990, 1991–1992, 1992–1993, 1995–1996, 1997–1998, 1998–1999, and 2005–2006. These years are chosen as part of a larger study [*Marshall and Scaife*, 2009; *Marshall et al.*, 2010; A. G. Marshall and A. A. Scaife, Improved predictability of Stratospheric Sudden Warming events in an AGCM with enhanced stratospheric resolution, submitted to *Journal of Geophysical Research*, 2009] that investigates the seasonal predictability of European surface winter climate anomalies associated with SSWs, QBO events, ENSO episodes, and volcanic eruptions. Fifteen-member ensembles for each winter period are initialized at 6-hourly intervals starting from 12Z on 27 November and ending with 00Z on 1 December to produce hindcasts that are integrated from a model start date of 1 December. The initial atmospheric conditions for each hindcast use data from the ERA-40 reanalysis. Each model experiment is forced with time-varying boundary conditions from greenhouse gases including CO2, CH4, N2O, CFCl3 and CF2Cl2 (specified at decadal intervals and interpolated linearly), and changes in vegetation, sulphur, soot, and biomass emissions. Sea surface

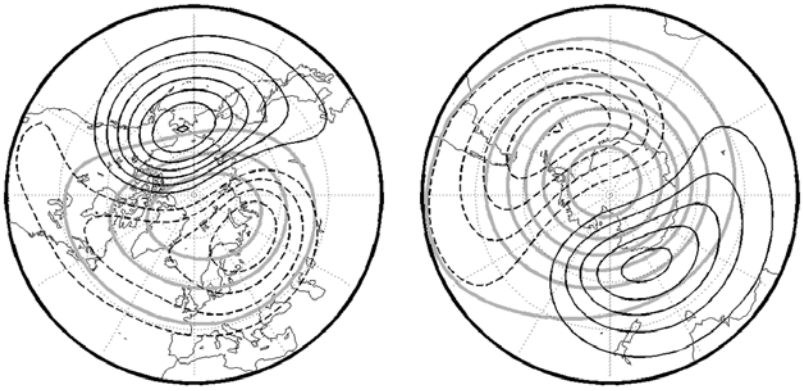

**Figure 1.** The deviation of the climatology of Z10 from its zonal mean in ERA-40 for NDJFM in the Northern Hemisphere and ASON in the Southern Hemisphere. Contours are drawn every 100 m with negative (cyclonic) contours dashed and the zero contour omitted. The thick shaded lines show the full climatology contoured every 500 m starting from 29.5 km in the Northern Hemisphere and 28.5 km in the Southern Hemisphere.

temperature and sea ice extent variations are specified from an analysis of historical observations [*Rayner et al.*, 2003], and atmospheric ozone concentrations were held constant at 1990 levels. Explosive volcanic eruptions are absent from the model simulations to avoid their masking effects on the extratropical circulation (Marshall and Scaife, submitted manuscript, 2009).

### 2.2. Stratospheric Variability

[10] To characterize stratospheric variability we perform an Empirical Orthogonal Function (EOF) analysis of daily geopotential height at 10 hPa (Z10), since this field is available for both the ERA-40 and the model data. Since Z10 varies on large scales only, the ERA-40 data were subsampled to a resolution of 2.25° to reduce processing time. The data were linearly detrended and a smooth seasonal cycle was removed, which was defined by averaging the data over all years and then applying a discrete cosine transform, retaining only the mean value and the two lowest cosine modes. An extra 15 days on either side of the seasons of interest were included in the transform to minimize edge effects. EOF analysis was then applied directly to the resulting daily Z10 anomaly data over the region poleward of 20°N, after weighting by the square root of the cosine of the latitude, as is conventional [*Baldwin et al.*, 2009]. We have tested the sensitivity of the results to changes in this method, for example by using a running mean to smooth the seasonal cycle and by not detrending the data before calculating the EOFs. These changes resulted in only very small quantitative changes in the correlation values obtained.

[11] It is useful to compare the EOF patterns to the zonal asymmetries of the time mean flow, so these asymmetries are shown in Figure 1. In these maps the zonal asymmetries are of similar magnitude in both hemispheres, but the zonal flow is stronger in the Southern Hemisphere, so the asymmetries represent weaker disturbances than those in the Northern Hemisphere. The same applies to the EOF patterns obtained, which also feature Z10 anomalies of similar magnitudes in both hemispheres.

### 2.3. Blocking Index

[12] Blocking is an anomalous synoptic pattern in which the prevailing westerlies and midlatitude storms are "blocked" by a large-scale, persistent anticyclone. In winter these events often bring severe cold to regions whose winter climate is normally moderated by a mild maritime influence. As described by *Pelly and Hoskins* [2003] the onset of blocking is associated with the breaking of a synoptic-scale Rossby wave in the upper troposphere. Following this perspective, we identify blocking events in both the reanalysis and model data using the two-dimensional index described by *Berrisford et al.* [2007]. This index identifies blocking episodes via the associated wave breaking, by searching for a reversal in the meridional contrast of potential temperature $\theta$ on the dynamical tropopause (the PV2 surface). At each point, $\theta_{PV2}$ is averaged over two boxes of 5° longitude by 15° latitude, to the north and south of the point. When the value of the northern box minus the southern box becomes larger than zero, a reversal is defined. Temporal and spatial scales are then applied to ensure that the events identified are large-scale, quasi-stationary and persistent (lasting at least 5 days), and these are then termed episodes. See *Berrisford et al.* [2007] for more details. It is these blocking episodes that we use to characterize blocking activity in this paper.

[13] The index is a straightforward two-dimensional extension to that of Pelly and Hoskins, in that blocking can be identified at all latitudes and longitudes. The index is usually applied every 4° between the latitudes of 25° and 73°. However, in the Northern Hemisphere the northernmost events are generally weak, since the mean meridional gradient there is weak, and so relatively easy to overturn [*Woollings and Hoskins*, 2008]. Approaching the tropics the PV2 surface becomes more elevated, and so missing or unrealistic values of the diagnosed potential temperature are common. This occurs at slightly higher latitudes in the model data, so the blocking index is only applied poleward of 37° in this data. The index is referred to in general as a wave-breaking index, and identifies events in midlatitudes

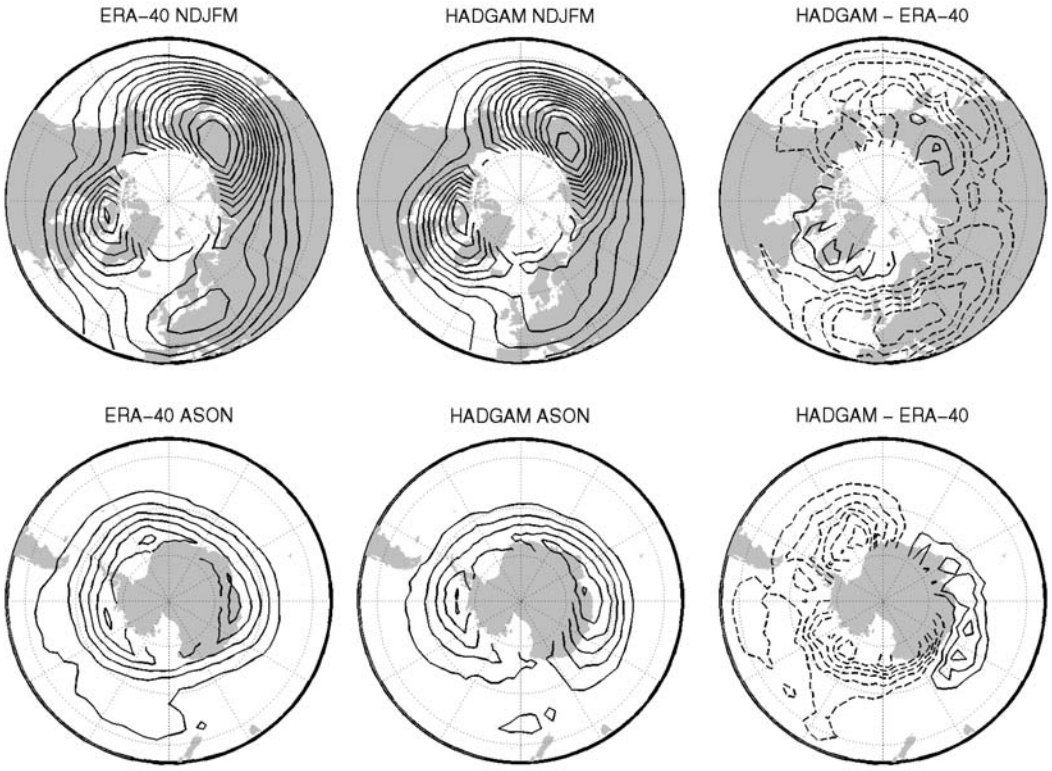


**Figure 2.** Maps of the climatological blocking episode frequency in ERA-40 and HadGAM for the (top) Northern and (bottom) Southern Hemisphere. The frequency is contoured every 0.05 day$^{-1}$, except in the two rightmost panels, which show the difference between HadGAM and ERA-40, contoured every 0.02 day$^{-1}$ with negative contours dashed and the zero contour omitted.

classed as blocking, and events on the poleward side of the storm tracks which are often termed high-latitude blocking.

[14] The climatological frequency of blocking episodes in the ERA-40 and HadGAM data is shown in Figure 2, for the chosen active seasons in both hemispheres. Blocking in the Northern Hemisphere is concentrated over Europe and two regions of frequent high-latitude blocking centered upstream of the two ocean basins. The model simulates the general structure of the climatology well but, in common with other GCMs, it does tend to underestimate the occurrence of blocking, especially over Europe and in the Pacific sector. In the Southern Hemisphere the occurrence of blocking is less geographically concentrated. Again the model climatology is generally good, although blocking is underestimated in the vicinity of the Weddell and Ross seas.

### 2.4. Wave Activity Diagnostic

[15] Flow variability in the stratosphere is largely driven by the upward propagation of long planetary-scale Rossby waves from the troposphere. To give insight into the mechanisms responsible for correlations between stratospheric variability and blocking we use a diagnostic measure of this Rossby wave activity. As described by *Vallis* [2006] the Eliassen-Palm relation

$$\frac{\partial A}{\partial t} + \nabla \cdot \mathbf{F} = D \tag{1}$$

is a conservation law for the wave activity density $A$, where $\mathbf{F}$ is the Eliassen-Palm flux and $D$ represents sources and sinks due to nonconservative terms. Here we use the wave activity density $A$ as a diagnostic of wave activity. $A$ can be calculated from the quasi-geostrophic potential vorticity $q$ using the relation

$$A = \frac{\overline{q'^2}}{2\partial\overline{q}/\partial y}, \tag{2}$$

where an overbar denotes a zonal mean and a prime denotes a deviation from this mean. $A$ therefore directly measures the potential vorticity variations that underlie Rossby wave activity, so is a natural diagnostic to choose. The potential vorticity on pressure surfaces is given by

$$q = f + \nabla^2\psi + \frac{\partial}{\partial p}\left(\frac{f_0^2}{S^2}\frac{\partial\psi}{\partial p}\right), \tag{3}$$

where the quasi-geostrophic stream function $\psi$ can be calculated from the geopotential $\phi$ by $\psi = \phi/f_0$. For the calculations here, the stream function was area-averaged over boxes of 5 × 5 cells on the ERA-40 1.125° grid in order to reduce the small-scale noise introduced by the derivatives in 3. Our interest is ultimately in the longest planetary wave numbers, so this level of "coarse graining" is justified.

[16] For the analysis performed here, we use the stability parameter

$$S^2 = -\frac{R}{p}\left(\frac{p}{p_R}\right)^{\kappa}\frac{d\theta}{dp} \quad (4)$$

for a reference isothermal profile of temperature $T = 250$ K. The potential temperature $\theta$ is given by $T(p_R/p)^{\kappa}$, with $\kappa = R/c_p = 287/1004$ and $p_R = 1000$ hPa. The denominator of equation (2) is calculated from the climatological mean $q$ in order to remove a few near-singular points from the data, and also to maintain consistency with the theory, in which $\overline{q}$ does not vary with time.

[17] In section 4 we composite the wave activity density $A$ for blocking events in different regions. $A$ is calculated every 5° of latitude between 40° and 80° and then area averaged over this latitude band for presentation. Examination of individual cases suggests that the area averaging compensates for changes in the latitude of wave activity in the troposphere. Wave activity for different zonal wave numbers is obtained by Fourier filtering using an FFT algorithm at each latitude separately before area averaging. The wave activity density is then linearly detrended and a seasonal cycle is removed, which is calculated by averaging over all years and then smoothing with a 7 day running mean.

[18] Although the seasonal cycle of $A$ is removed, the stationary waves still contribute to $q'$, and so to variations in $A$, depending on how the flow anomalies on any particular day interfere with the stationary waves. In order to determine whether the anomalies associated with blocking interfere positively or negatively with the stationary wave pattern, a second version of the wave activity density was also calculated with the contribution of the stationary waves removed. This was achieved by removing the stationary part of the $q$ field from each daily field prior to the evaluation of equation (2), where the stationary part was defined as the climatological seasonal mean of $q$.

## 3. Correlation Analysis

[19] In this section we demonstrate the existence of stratosphere-blocking links by correlating the principal components of the leading daily Z10 EOFs with the occurrence of blocking. Figure 3 shows the Northern Hemisphere EOF patterns alongside correlation maps of blocking with the principle component time series, for both the ERA-40 and HadGAM data. The ERA-40 EOF patterns comprise a wave number 0 pattern as the first EOF, then two wave number 1 patterns and two wave number 2 patterns in the subsequent EOFs. Comparison with Figure 1 shows how the EOF patterns modify the stationary wave pattern. For example, changes in the amplitude of the stationary waves are represented by EOF 2 along with contributions from the wave number 2 patterns. The dynamical relevance of EOF patterns is always questionable, especially for the higher EOFs. The patterns are clearly a convenient basis for describing zonal mean and wave number 1 and 2 variability, with two orthogonal wave patterns representing each zonal wave number, as in Fourier analysis. However, the patterns are also reminiscent of typical stratospheric flow patterns, especially for the wave number 1 and 2 patterns. In particular, the orientation of EOF patterns is very close to the stratospheric variability observed during minor and major warmings [e.g., *Matthewman et al.*, 2009]. The first three HadGAM EOFs are very similar to their observed counterparts and they explain similar fractions of variance. However, the patterns for EOFs 4–6 suggest that the model underestimates the amount of wave number 2 variability in the stratosphere, as seen in other stratosphere resolving GCMs [*Charlton et al.*, 2007].

[20] The correlation maps in Figure 3 show the correlations between the principle component time series and the blocking episode index at each location. The blocking episode index is binary, simply equalling one when a blocking is detected and zero otherwise. Correlations with lags of up to plus or minus one month have been calculated, but in most cases the instantaneous correlation maps are representative of the strongest relations seen, so only these are shown here. The exceptions to this are the correlations with EOF1, which are discussed later in this section. Note that the blocking index identifies the point of reversal of the meridional gradient of $\theta_{PV2}$, so that the anticyclone lies to the north of the point where correlations are observed. Local significance at the 95% level is determined using a $T$ test with an estimated sample size derived from the lag-1 autocorrelations of the two time series, as in the work of *Woollings et al.* [2008]. Field significance is then determined by a Monte Carlo approach using 500 trials in which the 44 years of stratospheric data are shuffled, keeping each season intact. This method gives an estimate of the number of grid cells at which the pointwise $T$ test is expected to be satisfied purely by chance, and the resulting two-sided field significance (FS) value is given alongside each correlation map.

[21] It is clear from Figure 3 that there are indeed several different stratosphere-blocking links, with very high levels of significance. Furthermore, many of these links are reproduced very well in the HadGAM data set, with equally high significance. It seems likely that the existence of several different links involving different blocking regions has contributed to previous contradictory results in the literature. In section 4 we will examine some of these links individually, region by region. For now, we just give an overview of the regional details of Figure 3, remembering that the sign of EOF patterns is arbitrary, so from this analysis it is not clear whether, for example, increased blocking accompanies the EOF2 pattern or decreased blocking accompanies its inverse.

[22] Interestingly it is the wave number 1 and 2 EOFs which show the strongest correlations, although the zonally symmetric EOF1 does correlate with high-latitude blocking over Greenland and Alaska. In addition to EOF1, blocking in the Greenland region is correlated to wave number 1 and 2 variability in the stratosphere, in both of the data sets. In contrast, correlations with blocking over Alaska are generally weak, with most of the significant correlations in the Pacific occurring upstream, in what we will refer to as the West Pacific. Note that north-south dipoles in blocking activity, such as that seen to be related to the ERA-40 EOF4 over the West Atlantic/Greenland, most likely indicate variations in blocking in the southern region where blocking occurs more rarely. When a block does occur in the vicinity of the southern center of the dipole an anticyclone lies to

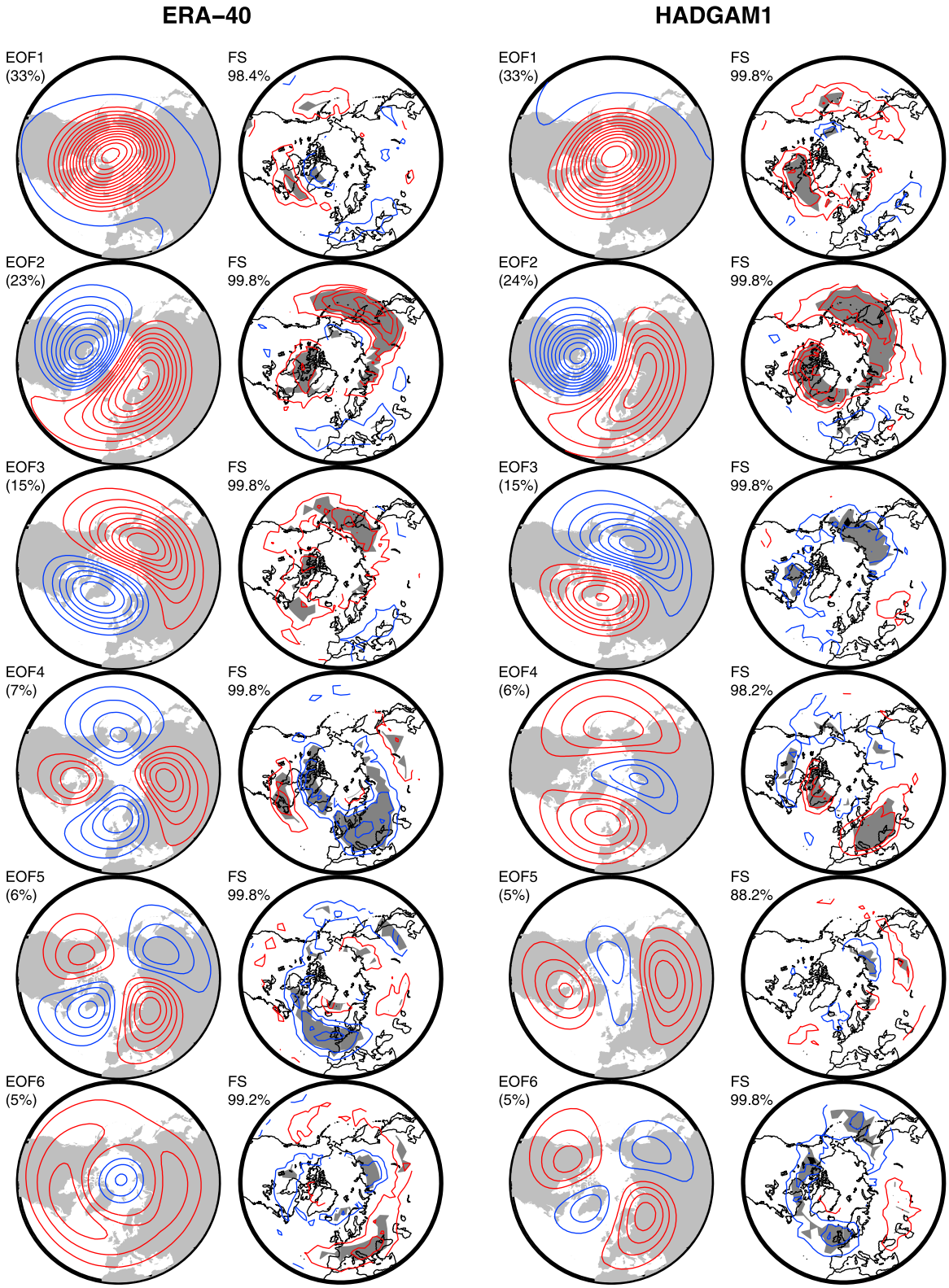


**Figure 3.** The six leading empirical orthogonal functions (EOFs) of daily Z10 (in the season NDJFM), and next to each EOF, the associated blocking episode instantaneous correlation map for both (left) ERA-40 and (right) HadGAM. The EOFs are displayed by regressing the Z10 anomalies onto the principal component time series and are contoured every 50 m. Correlations are contoured every 0.05, with significance at the 95% level indicated by shading. In all plots, negative contours are colored blue, and the zero contour is omitted. The fraction of variance explained by each EOF is given above and left of its map, and the field significance for the correlations maps is given above and left of each map.

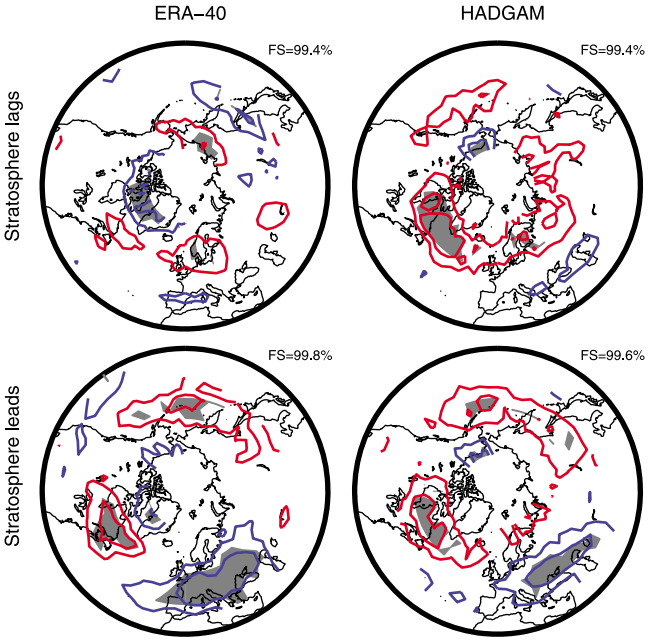


**Figure 4.** Six day lag correlation maps of Northern Hemisphere blocking with the first Z10 EOF in both the ERA-40 and HadGAM data sets. Contouring is as in Figure 3.

the north of this, so that the $\theta_{PV2}$ gradient is unlikely to be reversed in the vicinity of the northern center.

[23] Blocking over Europe is correlated with wave number 2 variability in the stratosphere, as described by EOFs 4 and 5 in the ERA-40 data. It is interesting that the phase difference between the two EOFs is also seen in the two correlation maps, with the EOF5 European blocking correlations located roughly 45° west of the EOF4 correlations. There is also a link between blocking over Southern Europe and the more zonally symmetric EOF6. This is similar to the results of *Santos et al.* [2009] who document stratospheric flow variations linked with strong ridge episodes over the eastern North Atlantic.

[24] As a test of robustness, we have repeated the analysis using height data at 70 hPa rather than 10 hPa (not shown). The resulting EOF patterns are similar, although the wave number 1 patterns are shifted about 30° to the east. The wave number 0 and 1 patterns have relatively smaller fractions of the variance at this level. Analysis of this data gives very similar correlation maps to those in Figure 3, although the correlations are generally stronger, as might be expected. The only feature which is qualitatively different from Figure 3 is that the 70 hPa EOF3 shows significant correlations with blocking over Northern Europe. This may reflect the fact the EOF3 pattern is phase shifted so that its Atlantic center lies closer to Europe. The results of sections 4.1 and 5 confirm that European blocking is linked to stratospheric disturbances of both wave number 1 and 2.

[25] The correlation patterns seen in the HadGAM data are generally similar to those in ERA-40, which gives further confidence to the results. The agreement is very good for EOFs 1–3 especially. For EOFs 4–6 there are correlations over Europe and the Atlantic in the same regions as seen in the ERA-40 maps, even though the structure of the individual EOFs are different. It is interesting that there is a link between European blocking and stratospheric wave number 2 variability, as these are both underrepresented in the model simulation. It is possible that the lack of European blocking could contribute to the lack of wave number 2 variability in the model's stratosphere.

[26] As stated above, the instantaneous correlation maps are generally representative of all the relations seen, but the exception to this is the relation with the first EOF. The instantaneous correlations in Figure 3 show links with the West Atlantic and the East Pacific, but lag correlations also exist with blocking over Europe. This is clear in 6 day lag correlation maps shown in Figure 4. The two data sets agree well on the correlations when the stratosphere leads, with only small differences in the locations of some features. When the stratosphere lags the two data sets are in less good agreement. In ERA-40 all of the correlations are stronger when the stratospheric variability leads the blocking index. These correlation patterns persist at similar magnitude for the stratosphere leading by up to 30 days (not shown). The correlations are also stronger when the stratosphere leads in the HadGAM data, with the exception of the correlations in the West Atlantic. Again, the correlations persist for much longer when the stratosphere leads, although only to around 20 days which is less than in the reanalysis. In contrast, correlation maps with the stratosphere lagging by more than 6 days are weak and incoherent in both data sets. Lag correlations by themselves do not prove that there is any physical causality with the stratosphere affecting the occurrence of blocking, but the contrast between the lead/lag maps in Figure 4 do provide encouraging evidence that there might be such a link. This is discussed further in the relevant regional analyses below.

[27] The correlation analysis has also been applied to the Southern Hemisphere in both data sets and the results are shown in Figure 5. As before, EOFs 1–5 represent variability in wave numbers 0–2. This time, however, the model EOFs are much more similar to those from ERA-40, although there are some phase differences, especially for the wave number 2 patterns. As before, the fractions of variance explained by the different patterns are very similar to those from ERA-40. The fact that wave number 2 variability is well represented here suggests that the underlying reason for lack of wave number 2 variability in the northern stratosphere lies in the troposphere.

[28] The correlation maps show that, while correlations are generally weaker than in the Northern Hemisphere, there are some stratosphere-blocking links with high field significance. In general, these are evident in both data sets, although the lower correlation values mean that in some cases the regions exhibiting significance do not precisely agree. The correlations only achieve field significance for the wave number 1 and 2 EOFs. As in the Northern Hemisphere, correlations with the zonally symmetric EOF1 are weaker, and in this case they are not significant. In contrast to the Northern Hemisphere the lag correlation structure for EOF1 is similar to that in the instantaneous map.

[29] Caution must be applied concerning the reliability of reanalysis data in the presatellite period, especially in the Southern Hemisphere. With this in mind, the correlation analysis has been repeated using only ERA-40 data from 1979 onward. In both hemispheres the main features of the

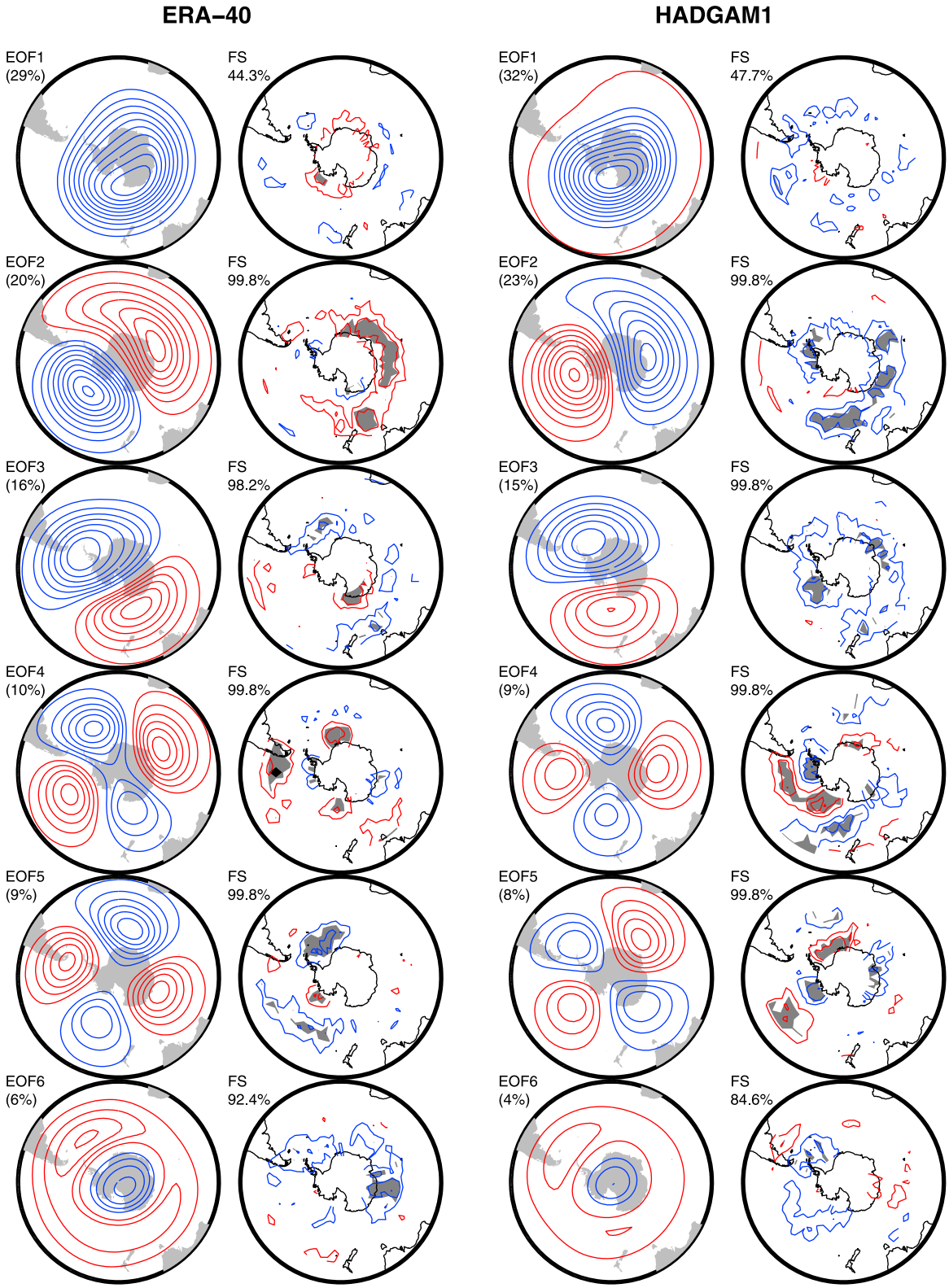


**Figure 5.** As in Figure 3, but for the Southern Hemisphere during ASON.

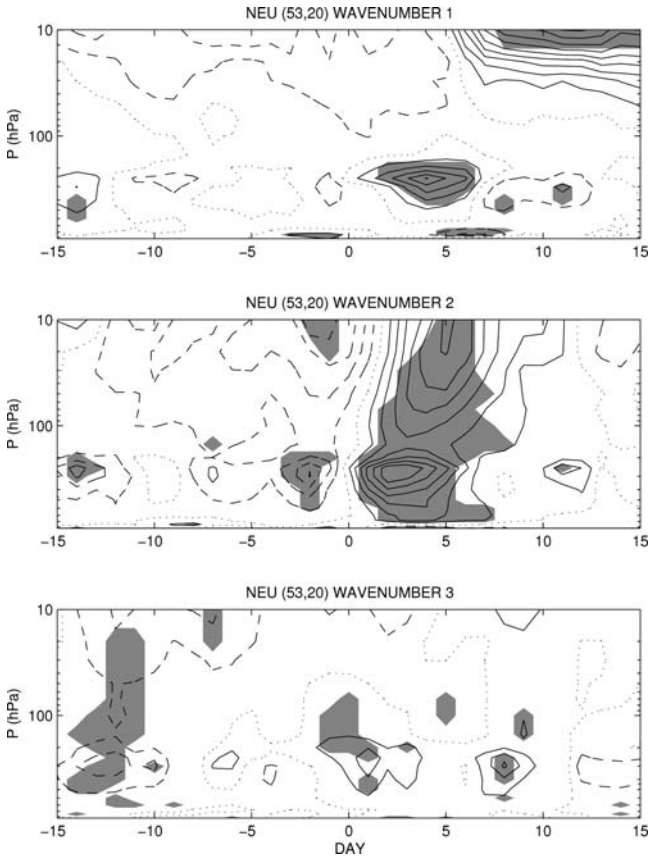


**Figure 6.** Time-pressure plots of area-averaged wave activity density anomalies in zonal wave numbers 1–3 composited with respect to the onset of blocking over Northern Europe (day 0), contoured every 0.01 $ms^{-1}$ with negative contours dashed and the zero contour dotted. Shading indicates values that are significant at the 95% level using a two-sided Monte Carlo test with 1000 trials in which the same number of "blocking onset days" is chosen at random. This is a composite of 136 events.

correlation maps and the levels of significance are very similar. This, along with the similarity to the results of the HadGAM analysis, suggest that the reduced observational coverage in the early years of ERA-40 has not adversely affected the analysis presented here.

## 4. Regional Analyses

[30] We now examine some of the strongest stratosphere-blocking links in more detail by forming composites with respect to the onset date of blocking events in certain key regions which are suggested by the correlation analysis. Blocking onset is defined as the first day which is part of a blocking episode after 5 consecutive days which are not. Owing to some limitations on data availability and for conciseness these regional analyses will be performed using the ERA-40 data only.

### 4.1. Northern Europe

[31] Northern Europe, lying at the end of the North Atlantic storm track, is the dominant midlatitude blocking region identified by this index. As shown in Figure 3, the significant simultaneous correlations here are associated with wave number 2 disturbances in the stratosphere. To give physical insight into the link we choose the location (53°N, 20°E) where high correlations with EOF4 are seen in Figure 3, and composite the wave activity density with respect to blocking onset at this point. The evolution of wave activity density anomalies (from the smooth seasonal cycle) is shown in Figure 6. The blocking anomaly itself is seen in the period immediately after day 0, and projects onto both wave numbers 1 and 2 in the troposphere. At later dates enhanced wave activity in these wave numbers is also evident in the stratosphere, with a particularly clear upward propagation of wave number 2 activity from the troposphere to the stratosphere. The wave number 1 disturbance develops in the uppermost stratosphere after the upward propagating pulse of wave number 2 activity reaches that level. This could indicate that the wave number 2 disturbance to the polar vortex decays into a wave number 1 disturbance, especially at uppermost levels, as often seen in the period following the split of the polar vortex during sudden warmings. There are some significant anomalies in wave activity preceding the blocking onset, especially in wave number 2 in the troposphere. This could reflect the existence of tropospheric flow precursors for European blocking, as described by *Nakamura et al.* [1997]. It could also be partly an artefact of the compositing, whereby the period immediately before onset by definition does not contain contributions from blocking.

[32] The blocking itself is a regional synoptic-scale disturbance, so we suggest that the large changes in tropospheric wave activity on the long planetary-scale wave numbers reflects the modification of the stationary wave pattern by the blocking anomalies. The stationary waves contribute to the wave activity density as shown in Figure 6, so to test this hypothesis we use the version of wave activity density calculated after removal of the climatological stationary waves from the data. For both wave numbers 1 and 2 the resulting composites (not shown) exhibit similar features in the troposphere as in Figure 6, but with much reduced amplitudes. This shows that the projection of the blocking anomaly onto these wave numbers interferes positively with the stationary waves, increasing the tropospheric wave activity, and this change then propagates upward into the stratosphere.

[33] Maps of the tropospheric and stratospheric flow evolution during Northern European blocking are shown in Figure 7. In the troposphere the blocking anomalies are clear over Europe, with no coherent features elsewhere. After the onset of blocking the stratospheric vortex shifts away from the Pacific and toward Eurasia, though note that EOFs of both wave number 1 and 2 contribute to this composite pattern. The enhancement of the Aleutian anticyclone in the stratosphere is typical of the flow evolution associated with sudden warmings. As shown in section 5, blocking over Northern Europe does emerge as a precursor to sudden warmings, in agreement with *Limpasuvan et al.* [2004], *Nishii et al.* [2009], *Martius et al.* [2009], E. W. Kolstad et al. (The association between stratospheric weak polar vortex events and cold air outbreaks, submitted to *Quarterly Journal of the Royal Meteorological Society*, 2009), C. I. Garfinkel et al. (Tropospheric precursors of anomalous Northern Hemisphere stratospheric polar vortices, submitted

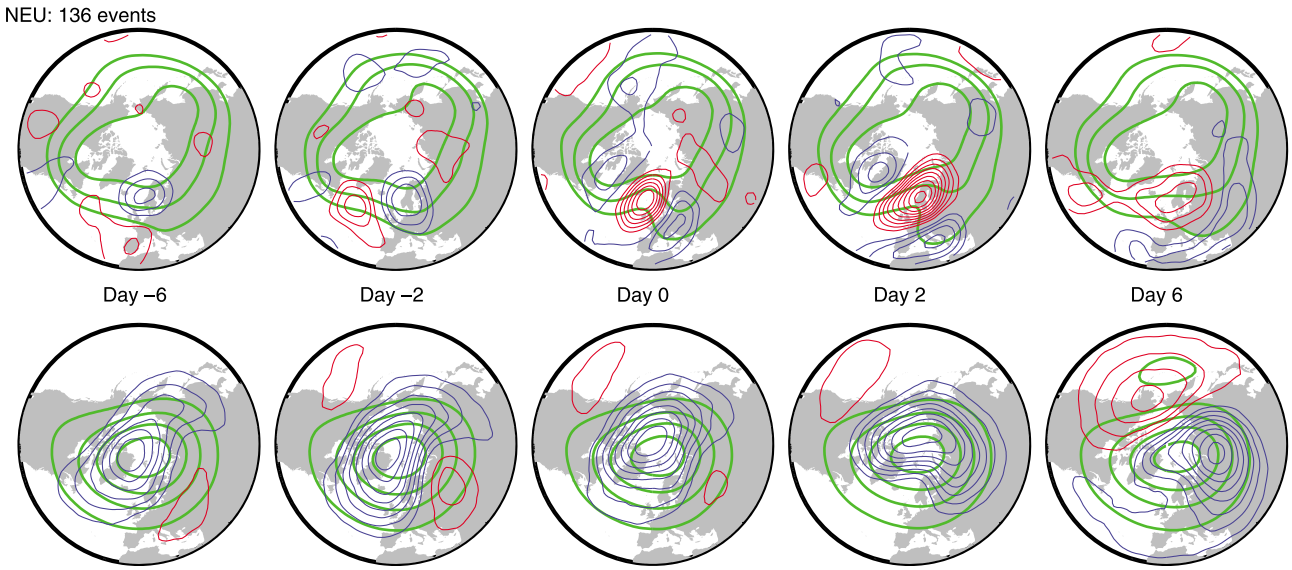


**Figure 7.** Flow evolution composited with respect to the onset of blocking over Northern Europe at day 0. (top) 250 hPa stream function anomalies from the time mean, contoured every $2 \times 10^6$ $s^{-1}$, with negative contours in blue and the zero contour omitted. To provide context, the composite full stream function field is shown by thick green contours every $2 \times 10^7$ $s^{-1}$ from $-9 \times 10^7$ $s^{-1}$ to $-15 \times 10^7$ $s^{-1}$. (bottom) 10 hPa geopotential height (Z10) anomalies contoured every 25 m, with negative contours in blue and the zero contour omitted. The composite full field is contoured in green every 500 m.

to *Journal of Climate*, 2009), and T. Breiteig (Tropospheric precursors of stratospheric warmings, submitted to *Climate Dynamics*, 2009).

[34] The composites also clearly show that the stratospheric vortex is anomalously strong in the period before blocking onset, reminiscent of the preconditioning of the vortex prior to sudden warmings [*McIntyre*, 1982; *Scott and Polvani*, 2004]. This feature is also evident in the correlation analysis, as shown in Figure 4. It is not clear whether this stratospheric lead represents any physical causality. Whenever the stratospheric vortex is disturbed there will be some projection onto EOF1, and since European blocking clearly perturbs the vortex this signal could simply reflect the absence of European blocking in the period before blocking onset.

[35] In Figure 3 it is apparent that there are different regions of Europe which exhibit slightly different correlations. However this analysis has been repeated for locations in Western and Southern Europe and the composite flow and wave activity anomalies are generally similar to those shown here.

### 4.2. Greenland

[36] Blocking over Greenland results in flow anomalies resembling the negative phase of the North Atlantic Oscillation (NAO), and in fact *Woollings et al.* [2008] suggested that much of the multiyear variability of the NAO is associated with variations in the occurrence of Greenland blocking. Evidence for a stratosphere-troposphere connection associated with the NAO [e.g., *Ambaum and Hoskins*, 2002; *Baldwin and Dunkerton*, 2001; *Marshall and Scaife*, 2009] could therefore be relevant to the correlations seen here.

[37] In Figure 3 there are instantaneous correlations between Greenland blocking and several of the EOFs, most clearly EOFs 1, 3, and 4. The composite flow evolution for these events is given in Figure 8. In contrast to European blocking the stratospheric vortex is anomalously weak in the period prior to blocking onset. This is supported by lag correlation analysis, which shows significant correlations between blocking and EOF1 when the EOF leads by around a week (Figure 4). This is consistent with the analysis of Woollings et al. and the literature cited above which suggests a downward propagation of annular mode anomalies from the stratosphere to the troposphere.

[38] After the onset of blocking the stratospheric vortex is distorted, with a fairly complex composite anomaly pattern. The wave activity density (not shown) exhibits weaker upward wave propagation than that associated with European blocking, although there is clear and significant upward propagation in wave number 3, which contributes to the complexity of the Z10 anomalies in Figure 8. Higher wave numbers such as this can only propagate upward when the stratospheric vortex is weak [*Charney and Drazin*, 1961], as is the case here. Comparing the two versions of wave activity density, those with and without the stationary waves, shows that in this case the tropospheric wave number 1 anomalies associated with the blocking interfere destructively with the stationary wave number 1 anomalies. This could explain the weaker upward wave propagation than associated with European blocking.

### 4.3. West Pacific

[39] Blocking in the West Pacific correlates particularly well with EOF2 (see Figure 3). The composite flow evolution for blocking at the representative location (49°N, 155°E) is shown in Figure 9. This does show stratospheric

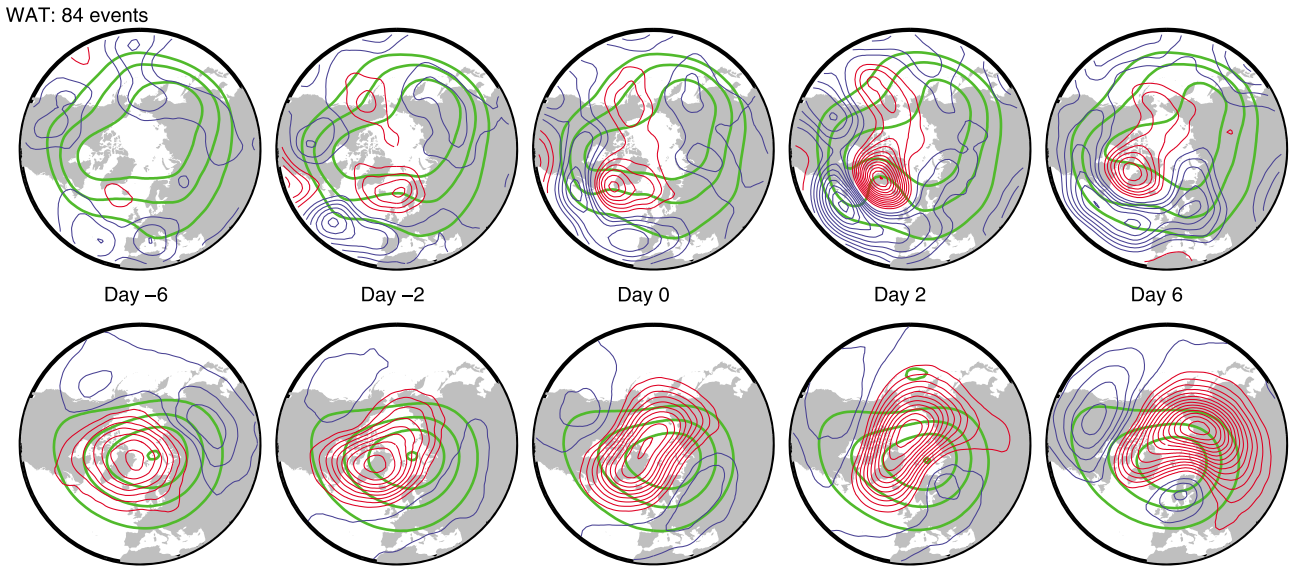


**Figure 8.** As in Figure 7, but for blocking at (53°N, 50°W) in the West Atlantic, referred to here as Greenland blocking.

anomalies before blocking onset, but these are much weaker than those after onset, when the vortex shifts toward Canada in a reduction of the climatological stationary wave amplitude.

[40] The wave activity density (Figure 10) tells a similar story. Blocking is associated with an increase in tropospheric wave number 2 activity which propagates up into the stratosphere. However, in wave number 1 the composite shows opposite behavior in the stratosphere and the troposphere: an increase in wave activity in the troposphere but a decrease in activity propagating upward through the stratosphere. Again, this difference can be understood by considering the interaction with the stationary waves. If the stationary waves are removed before calculating the wave activity density the picture is changed significantly, and this is shown in Figure 11. Now the wave activity anomaly is positive in both the troposphere and stratosphere, with the anomaly propagating up into the stratosphere. This suggests that West Pacific blocking is associated with a wave number 1 disturbance which propagates upward from the troposphere into the stratosphere. However, in the stratosphere this disturbance interferes destructively with the stationary wave pattern, so the vortex becomes more zonal, with lower total wave number 1 wave activity. This is consistent with the results of *Limpasuvan et al.* [2005], who show that an anticyclonic anomaly in this region tends to precede stratospheric vortex intensification events.

### 4.4. Southern Hemisphere

[41] In the Southern Hemisphere, correlations between blocking and stratospheric variability are weaker, probably because the stationary waves are weaker and the strato-

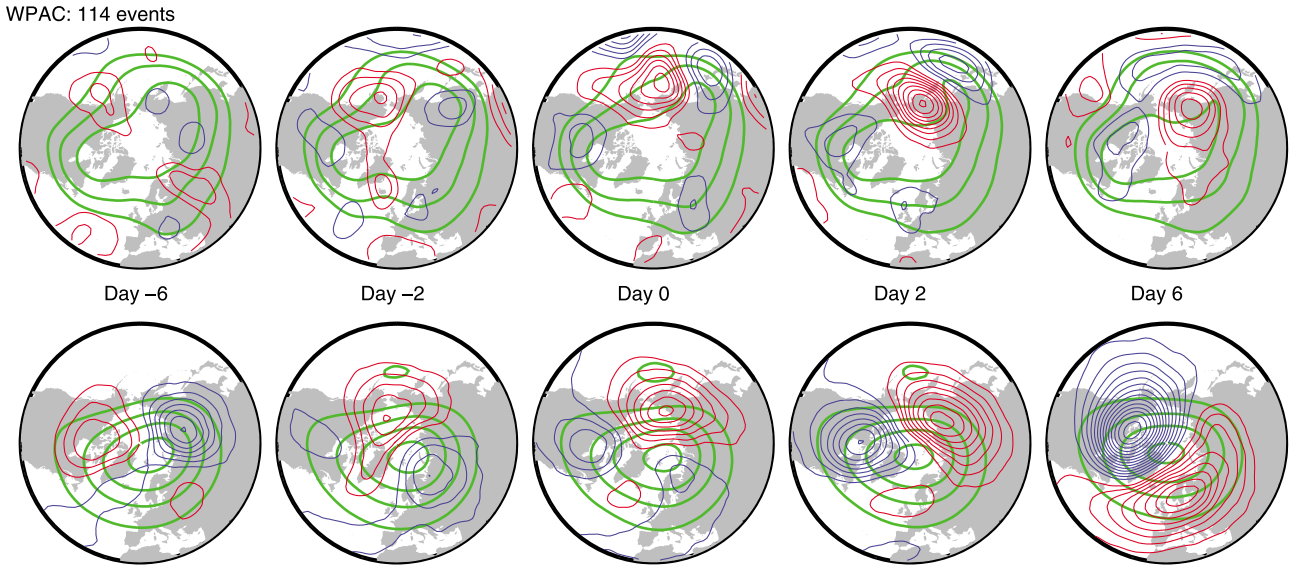


**Figure 9.** As in Figure 7, but for blocking at (49°N, 155°E) in the West Pacific.

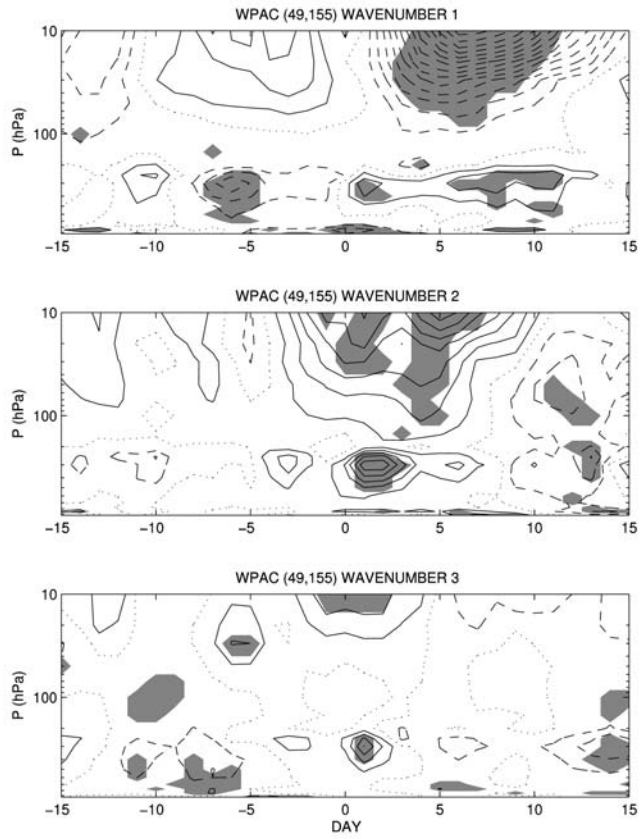


**Figure 10.** As in Figure 6, but for 111 events with blocking at (49°N, 155°E) in the West Pacific. There are slightly fewer events in this composite than that of Figure 9 as the inclusion of longer lag periods increases the restriction of data availability.

spheric vortex is stronger. However, there are significant links often exhibiting behavior similar to that in the Northern Hemisphere. Here we just show one example, that of blocking in the vicinity of New Zealand, as characterized by the point (53°S, 160°E). Blocking in this region is very rare, with only 16 events in the season 16 August–15 November which is used to composite wave activity density. These events all occur in the period after 1975, which gives rise to doubts over the ability of ERA-40 to represent these events in the absence of satellite data. However, blocks in this region are among the most similar to the classical midlatitude blocking seen in the Northern Hemisphere [*Berrisford et al.*, 2007].

[42] The wave activity composites for these events are shown in Figure 12. There is a clear upward propagation of wave number 2 activity in the period after blocking onset, similar to that seen in association with European blocking. This signal is clearer than that of wave number 1, despite the correlations with EOFs 2 and 3 in Figure 5. Flow composites (not shown) exhibit a more complicated pattern of anomalies involving both wave numbers 1 and 2, which may account for this discrepancy.

[43] There is also a large increase in wave number 3 activity in the troposphere appearing as a precursor to the blocking. This is also evident at several other blocking locations which have been examined. The Southern Hemisphere troposphere is known to exhibit strong wave number 3 variability [*van Loon and Jenne*, 1972; *Mo and White*, 1985; *Kidson*, 1988; *Karoly*, 1989] and there is evidence that this variability can influence the occurrence of blocking [*van Loon*, 1956; *Trenberth and Mo*, 1985; *Renwick and Revell*, 1999]. This may in fact be of relevance to the stratosphere-blocking link. In this composite, the preexisting tropospheric wave number 3 anomaly vanishes at the onset of blocking and is replaced by anomalous activity of wave numbers 1 and 2. It appears that the blocking anomaly modifies the preexisting wave number 3 pattern so that it projects instead onto the longer wavelengths, which are then more able to propagate upward into the stratosphere. Note that Figure 12 shows the wave activity with the effect of stationary waves removed. This makes very little difference to the results, suggesting that the stationary waves are not important for this process.

## 5. Sudden Warmings

[44] Correlating the blocking index with time series of stratospheric variability has enabled us to identify clear and highly significant links between the two. Now we examine the periods around observed sudden stratospheric warmings to see if there are signals in blocking which match the

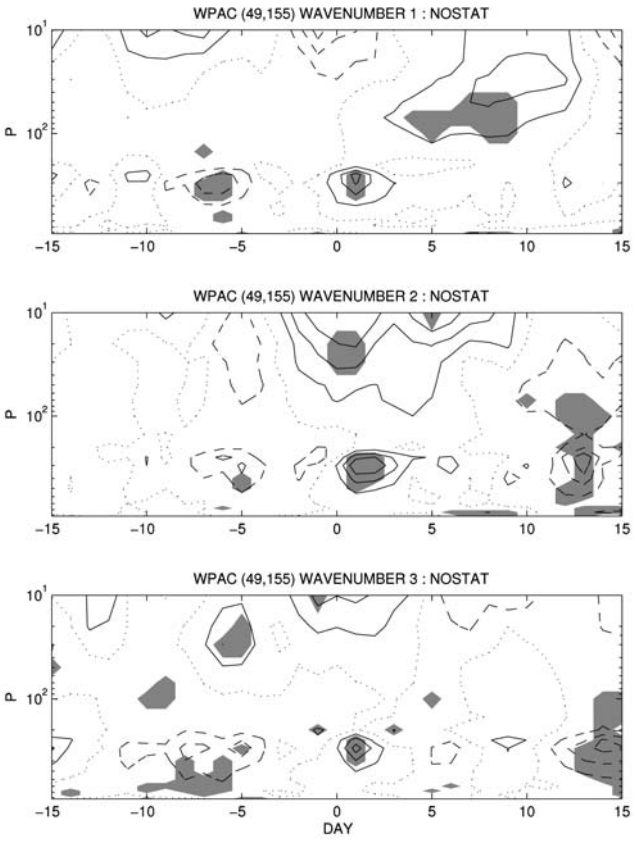


**Figure 11.** As in Figure 10, but with the stationary waves removed before calculation of the wave activity density.

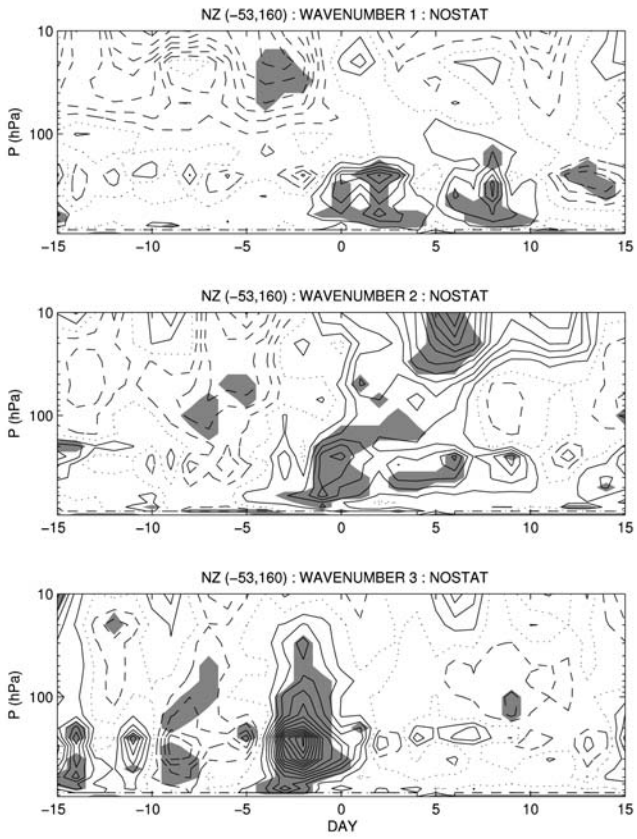


**Figure 12.** As in Figure 11, but for 16 events with blocking at (53°S, 160°E), in the vicinity of New Zealand.

relations already noted. We show in Figure 13 the blocking episode frequency anomaly composited with respect to the central date of sudden warmings in ERA-40, as given by *Charlton and Polvani* [2007]. Field significance is generally low in these composites, reflecting the small sample size, but in some cases the blocking anomalies seen here are in agreement with the analyses of sections 3 and 4, increasing confidence in these links. (The data needed to calculate the blocking index is not available for the event in 2002, leaving 14 split and 14 displacement events.)

[45] For example, there is increased occurrence of European blocking in the period before sudden warmings, especially for displacement warmings, which is in agreement with the upward propagation of wave number 1 and 2 anomalies seen in Figure 6. This is supported by the studies cited in section 4.1. The occurrence of European blocking is then reduced in the period after the central date of the warming. The mechanism responsible for this is not clear, but a reduction in European blocking in the period after a weakening of the stratospheric vortex is consistent with the lagged correlation analysis in Figure 4.

[46] After split vortex warmings there is increased blocking over both the Atlantic and Pacific basins, which is again consistent with the correlations in Figure 4 with a weakening of the vortex (positive EOF1) leading the blocking. The evolution of these composites is very similar to that proposed by *Woollings and Hoskins* [2008] to explain the weak tendency for high-latitude blocking to occur over both basins at the same time. Blocking occurs simultaneously over both the western North Atlantic and the East Pacific as the stationary wave trough over Canada is deformed, and then the blocking anomaly shifts upstream in the Pacific. This results in a tropospheric anomaly pattern resembling the negative phase of the NAM, and Woollings and Hoskins showed that these events do tend to occur in association with split warming events.

[47] The recent winter of 2008/09 was notable for a split vortex sudden warming of unprecedented amplitude [*Manney et al.*, 2009], so we briefly examine the occurrence of blocking in this winter for events which match the relationships described above. This winter is outside the ERA-40 period, so its events do not contribute to the results presented so far. Figure 14 shows a Hovmöller plot summarizing the blocking activity in this winter. The central date of the sudden warming was 24 January, corresponding to day 55. The warming was preceded by a blocking event over Europe by around 15–20 days. Figure 13 does show increased European blocking 11–20 days before split warmings and, although this does not pass the significance test, the results of the correlation and wave activity analyses support the view that European blocking leads to the upward propagation of wave number 2 activity into the stratosphere. Ten to 20 days before the warming there was also a persistent blocking episode at 150°E–180°E over the West Pacific, a precursor more usually associated with displacement warmings. There is another such event 10–20 days after the warming, which is in agreement with the composites. To summarize, this winter exhibited clear examples of some of the features identified in the composite analysis above, in particular the tendency for European blocking to precede split warmings as well as displacement warmings.

[48] This winter is also instructive with regard to the role of the East Pacific in sudden warmings. *Martius et al.* [2009] recently presented evidence that split warmings are often preceded by blocking over the East Pacific. There is evidence of this in Figure 13, but the region does not emerge as one with significant correlations with the stratospheric EOFs in Figure 3. Figure 15 shows $\theta_{PV2}$ for the 12 January, i.e., 12 days prior to the central date of the sudden warming. The European blocking is easily identified as a reversal of the meridional gradient of potential temperature associated with a large anticyclonic wave breaking. In the East Pacific there is also a large-scale ridge but this is oriented meridionally and does not exhibit the reversed gradient which is the signature of wave breaking. One of the key differences between our blocking index and that used by Martius et al. is that our index does not consider this to be a block since it is not related to a wave breaking event. Tropospheric flow features of all kinds, such as ridges, troughs and wave trains, can clearly modify the large-scale planetary waves and so influence the stratosphere. However, this paper specifically focuses on blocking, which is a particular dynamical event associated with the breaking of synoptic-scale Rossby waves, and as such is distinct from other anticyclones [*Masato et al.*, 2009]. Regardless of this, it is encouraging that the appearance of this East Pacific ridge in the period

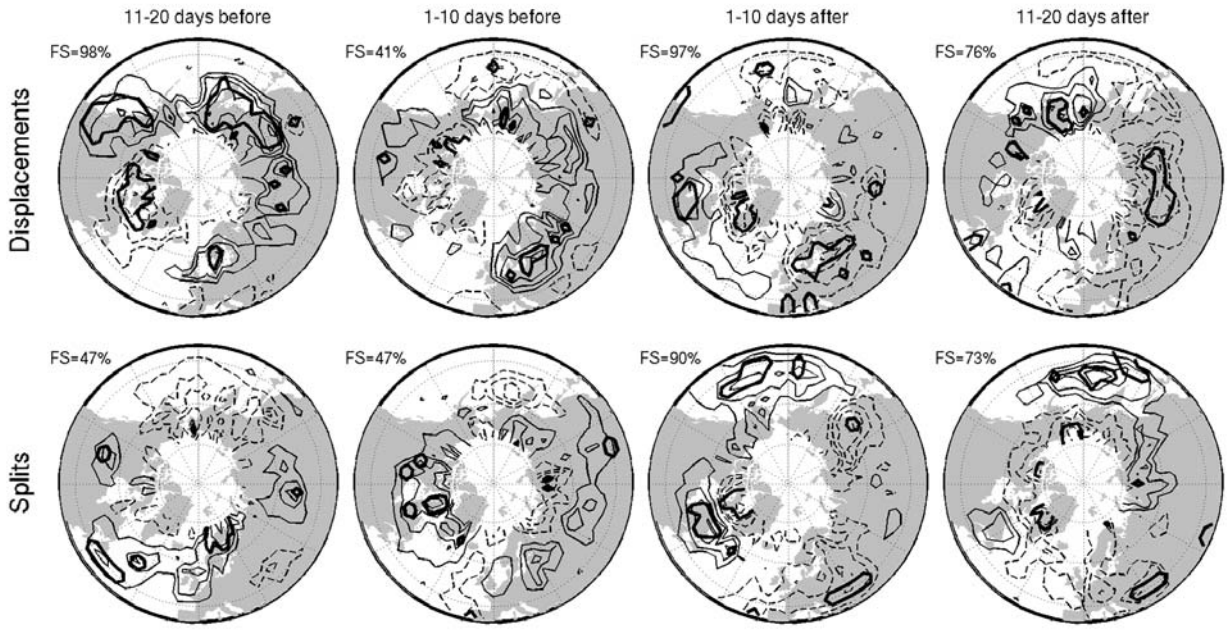


**Figure 13.** Composite anomalies of the blocking episode frequency in 10 day periods with respect to the central date of the sudden warmings in ERA-40. Contours are drawn every 0.05 day$^{-1}$ with negative values dashed and the zero contour omitted. A bold contour denotes significance at the 95% level in a two-sided Monte Carlo test using 1000 trials in which sudden warming dates are chosen at random. Field significance is determined by the fraction of these trials in which the pointwise test is passed over the same spatial area as in the observed composite.

before the 2009 split warming is in good agreement with the results of Martius et al.

## 6. Model Intercomparison

[49] One of the motivations for studying the stratosphere-blocking link is to determine whether improving the representation of stratospheric flow could reduce the long-standing problem of the underestimation of blocking in numerical models. *Scaife and Knight* [2008] recently gave an example of a climate model which did indeed show an increase in blocking when the number of model levels in the stratosphere was increased. Here we present a similar comparison using the model simulations described in section 2.1. We simply compare the mean blocking episode frequency in the 15-member ensembles of the 15 selected winters. This gives total ensemble sizes of 225 winters, although note that the period DJF is used for these ensembles rather than the extended period NDJFM used in the rest of this paper.

[50] The results of this comparison are summarized in Figure 16. As expected, compared to ERA-40 blocking is underestimated in the L38 ensemble, especially over Europe and the Pacific (Figure 16a). In contrast to the results of *Scaife and Knight* [2008] the occurrence of blocking is not increased in the L60 ensemble. Figure 16b shows that the difference in blocking occurrence between the two ensembles is small, especially over the main blocking regions, although the reduction in blocking over Asia does act to reduce the bias of the L38 model there. As in Scaife and Knight, the difference in blocking between the two ensembles can be explained by the difference in the tropospheric climatology (not shown; see Scaife and Knight for more details).

[51] This analysis shows that in general simply adding levels to a GCM will not necessarily improve the representation of blocking in the model. *Marshall et al.* [2010] showed that this model has reasonably realistic stratospheric variability, though it may be that further model development, for example of parameterizations, is needed to fully exploit the potential given by the increased number of levels. It is also possible, given the design of these ensembles, that some memory of the initial conditions may contribute to reducing the differences in blocking (see Marshall and Scaife, submitted manuscript, 2009).

## 7. Concluding Remarks

[52] In this paper we have shown that there are several different associations between stratospheric variability and tropospheric blocking. The use of an EOF-based approach through which the whole time series of stratospheric variability are used to calculate correlations is instrumental in identifying links with high statistical significance. When only the stratospheric sudden warming events are considered the field significance of the results is much lower. The existence of several different stratosphere-blocking links is likely to have contributed to the contradictory results on this issue presented in the literature.

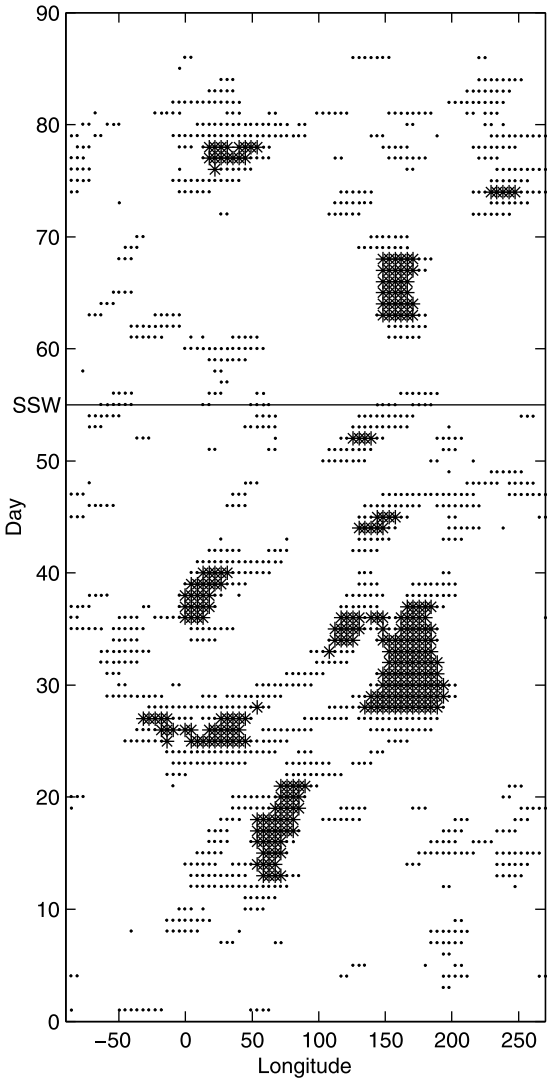


**Figure 14.** Hovmöller of blocking activity along 53°N for the winter season 2008–2009. Dots mark points exhibiting local and instantaneous blocking, and asterisks mark points considered part of a sector blocking episode, which indicates extent in both longitude and time (see *Berrisford et al.* [2007] for details). Note that for this plot only, the potential temperature was smoothed by a 15° running mean in longitude before applying the blocking index. The central date of the sudden warming is marked by a horizontal line.

[53] Correlations from ERA-40 have been compared to those from a simulation of an atmospheric GCM with a well resolved stratosphere. The model simulates both blocking and stratospheric variability reasonably well, apart from an underestimate of European blocking and of wave number 2 variability in the Northern Hemisphere stratosphere. Interestingly these two features are themselves related, so this stratospheric deficiency may be related to the lack of blocking. In general, however, correlation results from the model are very similar to those from ERA-40, increasing confidence in the reality of these associations.

[54] The occurrence of blocking is shown to modify the preexisting long planetary waves in the troposphere, resulting in upward propagation of these long wave anomalies into the stratosphere. The preexisting tropospheric planetary waves can be either stationary or transient, as seen in the Southern Hemisphere in the interaction of blocking with wave number 3 disturbances. In the Northern Hemisphere the modification of the stationary waves by blocking is critical for the effect on the stratosphere. European blocking is well positioned to interfere positively with both stationary waves 1 and 2, and emerges as a precursor to both displacement and split sudden warmings.

[55] While blocking influences the stratosphere via wave activity, the inverse influence of the stratosphere on blocking, if indeed there is one, is via the zonal mean flow, characterized here by the leading EOF. Correlations between the principal component time series of this EOF and the blocking index are stronger, more extensive and more significant when the stratosphere leads the blocking than vice versa. Significant stratosphere-leading correlations are seen with blocking over the West Atlantic, the Pacific and Europe (Figure 4). Blocking in the first two of these regions (often referred to as high-latitude blocking) results in flow anomalies similar to the negative phase of the NAO or the NAM, so these correlations seem to be further evidence of the downward propagation of annular mode variations from the stratosphere to the troposphere. These blocking events may constitute the transient eddy feedback which amplifies jet stream perturbations descending from the stratosphere [*Song and Robinson*, 2004]. Blocking over Europe is also related to the NAO, so the correlation in this region could also be a consequence of the downward NAO/NAM connection. However, given the magnitude and extent of the correlations over Europe it seems possible that the stratospheric zonal mean flow could be directly influencing the occurrence of European blocking.

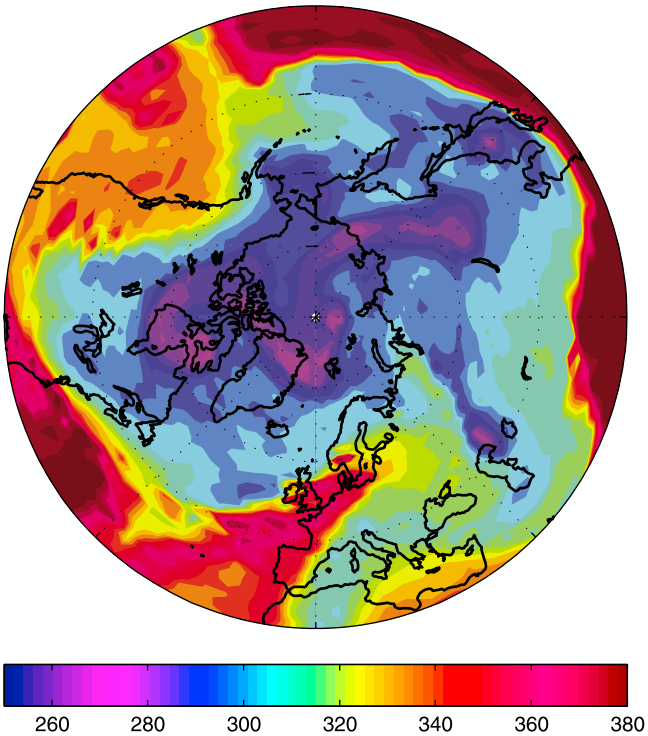


**Figure 15.** Daily mean $\theta_{PV2}$ for 12 January 2009.

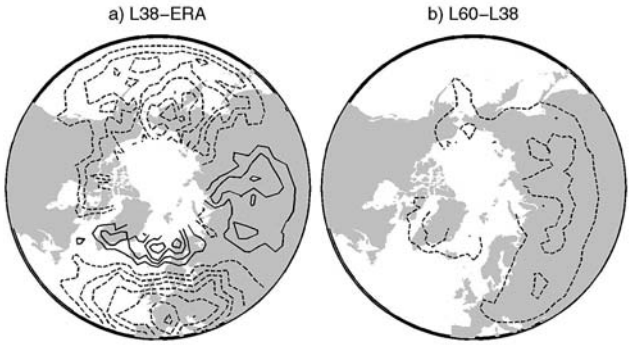


**Figure 16.** Differences in the DJF blocking episode frequency: (a) HadGEM2-A L38 ensemble minus ERA-40 and (b) L60 ensemble minus L38 ensemble. Contours are drawn every 0.02 day$^{-1}$ with negative contours dashed and the zero contour omitted.

[56] The underestimation of blocking is an enduring problem faced by numerical models, and this reduces confidence in model forecasts on all timescales from the medium-range upward. We have given an example in which increasing the number of model levels to improve the representation of stratospheric variability unfortunately does not improve the representation of blocking in the model.

[57] **Acknowledgments.** We are indebted to ECMWF for providing the ERA-40 Reanalysis and operational analysis data. S.I. and A.G.M. were supported by the Joint DECC and Defra Integrated Climate Programme, DECC/Defra (GA01101). We would also like to thank Brian Hoskins, Mike Blackburn, and Olivia Martius for useful discussions and the anonymous reviewers for their constructive comments.

## References

Ambaum, M. H. P., and B. J. Hoskins (2002), The NAO troposphere-stratosphere connection, *J. Clim.*, *15*, 1969–1978.

Andrews, D. G., J. R. Holton, and C. B. Leovy (1987), *Middle Atmosphere Dynamics*, Academic, San Diego, Calif.

Baldwin, M. P., and T. J. Dunkerton (2001), Stratospheric harbingers of anomalous weather regimes, *Science*, *294*, 581–584.

Baldwin, M. P., D. B. Stephenson, D. W. J. Thompson, T. J. Dunkerton, A. J. Charlton, and A. O'Neill (2003), Stratospheric memory and skill of extended-range weather forecasts, *Science*, *301*, 636–640.

Baldwin, M. P., D. B. Stephenson, and I. T. Jolliffe (2009), Spatial weighting and iterative projection methods for EOFs, *J. Clim.*, *22*, 234–243.

Berrisford, P., B. J. Hoskins, and E. Tyrlis (2007), Blocking and Rossby wave-breaking on the dynamical tropopause in the Southern Hemisphere, *J. Atmos. Sci.*, *64*, 2881–2898.

Black, R. X., and B. A. McDaniel (2007), Interannual variability in the Southern Hemisphere circulation organized by stratospheric final warming events, *J. Atmos. Sci.*, *64*, 2968–2975.

Charlton, A. J., and L. M. Polvani (2007), A new look at stratospheric sudden warmings. Part I: Climatology and modeling benchmarks, *J. Clim.*, *20*, 449–469.

Charlton, A. J., L. M. Polvani, J. Perlwitz, F. Sassi, E. Manzini, K. Shibata, S. Pawson, J. E. Nielsen, and D. Rind (2007), A new look at stratospheric sudden warmings. Part II: Evaluation of numerical model simulations, *J. Clim.*, *20*, 470–488.

Charney, J. G., and P. G. Drazin (1961), Propagation of planetary scale disturbances from the lower into the upper atmosphere, *J. Geophys. Res.*, *66*, 83–109.

Collins, W. J., et al. (2008), Evaluation of the HadGEM2 model, *Tech. Rep. 74*, Hadley Cent. Met Off., Exeter, U. K.

D'Andrea, F., et al. (1998), Northern Hemisphere atmospheric blocking as simulated by 15 atmospheric general circulation models in the period 1979–1988, *Clim. Dyn.*, *14*, 385–407.

Dole, R. M., and N. D. Gordon (1983), Persistent anomalies of the extratropical Northern Hemisphere wintertime circulation: Geographical distribution and regional persistence characteristics, *Mon. Weather Rev.*, *111*, 1567–1586.

Hinton, T. J., B. J. Hoskins, and G. M. Martin (2009), The influence of tropical sea surface temperatures and precipitation on north Pacific atmospheric blocking, *Clim. Dyn.*, *33*, 549–563.

Karoly, D. J. (1989), Southern Hemisphere circulation features associated with El Nino–Southern Oscillation events, *J. Clim.*, *2*, 1239–1251.

Kidson, J. W. (1988), Interannual variations in the Southern Hemisphere circulation, *J. Clim.*, *1*, 1177–1198.

Kodera, K., and M. Chiba (1995), Tropospheric circulation changes associated with stratospheric sudden warmings: A case study, *J. Geophys. Res.*, *100*, 11,055–11,068.

Labitzke, K. (1965), On the mutual relation between stratosphere and troposphere during periods of stratospheric warmings in winter, *J. Appl. Meteorol.*, *4*, 91–99.

Limpasuvan, V., D. W. J. Thompson, and D. L. Hartmann (2004), The life cycle of the Northern Hemisphere sudden stratospheric warmings, *J. Clim.*, *17*, 2584–2597.

Limpasuvan, V., D. L. Hartmann, D. W. J. Thompson, K. Jeev, and Y. L. Yung (2005), Stratosphere-troposphere evolution during polar vortex intensification, *J. Geophys. Res.*, *110*, D24101, doi:10.1029/2005JD006302.

Manney, G. L., M. J. Schwartz, K. Kryger, M. L. Santee, S. Pawson, J. N. Lee, W. H. Daffer, R. A. Fuller, and N. J. Livesey (2009), Aura Microwave Limb Sounder observations of dynamics and transport during the record-breaking 2009 Arctic stratospheric major warming, *Geophys. Res. Lett.*, *36*, L12815, doi:10.1029/2009GL038586.

Marshall, A. G., and A. A. Scaife (2009), Impact of the QBO on surface winter climate, *J. Geophys. Res.*, *114*, D18110, doi:10.1029/2009JD011737.

Marshall, A., A. Scaife, and S. Ineson (2010), Enhanced seasonal prediction of European winter warming following volcanic eruptions, *J. Clim.*, in press.

Martin, G. M., M. A. Ringer, V. D. Pope, A. Jones, C. Dearden, and T. J. Hinton (2006), The physical properties of the atmosphere in the New Hadley Centre Global Environmental Model (HadGEM1). Part I: Model description and global climatology, *J. Clim.*, *19*, 1274–1301.

Martius, O., L. M. Polvani, and H. C. Davies (2009), Blocking precursors to stratospheric sudden warming events, *Geophys. Res. Lett.*, *36*, L14806, doi:10.1029/2009GL038776.

Masato, G., B. J. Hoskins, and T. J. Woollings (2009), Can the frequency of blocking be described by a red noise process?, *J. Atmos. Sci.*, *66*, 2143–2149.

Matthewman, N. J., J. G. Esler, A. J. Charlton-Perez, and L. M. Polvani (2009), A new look at stratospheric sudden warmings. Part III. Polar vortex evolution and vertical structure, *J. Clim.*, *22*, 1566–1585.

McIntyre, M. E. (1982), How well do we understand the dynamics of stratospheric warmings?, *J. Meteorol. Soc. Jpn.*, *60*, 37–65.

Mo, K. C., and G. H. White (1985), Teleconnections in the Southern Hemisphere, *Mon. Weather Rev.*, *113*, 22–37.

Nakamura, H., M. Nakamura, and J. L. Anderson (1997), The role of high- and low-frequency dynamics in blocking formation, *Mon. Weather Rev.*, *125*, 2074–2093.

Nishii, K., H. Nakamura, and T. Miyasaka (2009), Modulations in the planetary wave field induced by upward-propagating Rossby wave packets prior to stratospheric sudden warming events: A case-study, *Q. J. R. Meteorol. Soc.*, *135*, 39–52.

O'Neill, A., W. L. Grose, V. D. Pope, H. Maclean, and R. Swinbank (1994), Evolution of the stratosphere during northern winter 1991/92 as diagnosed from U.K. Meteorological Office analyses, *J. Atmos. Sci.*, *51*, 2800–2817.

Pelly, J. L., and B. J. Hoskins (2003), A new perspective on blocking, *J. Atmos. Sci.*, *60*, 743–755.

Polvani, L. M., and D. W. Waugh (2004), Upward wave activity flux as a precursor to extreme stratospheric events and subsequent anomalous surface weather regimes, *J. Clim.*, *17*, 3548–3554.

Quiroz, R. S. (1986), The association of stratospheric warmings with tropospheric blocking, *J. Geophys. Res.*, *91*, 5277–5286.

Rayner, N. A., D. E. Parker, E. B. Horton, C. K. Folland, L. V. Alexander, D. P. Rowell, E. C. Kent, and A. Kaplan (2003), Global analyses of sea surface temperature, sea ice, and night marine air temperature since the late nineteenth century, *J. Geophys. Res.*, *108*(D14), 4407, doi:10.1029/2002JD002670.

Renwick, J. A., and M. J. Revell (1999), Blocking over the South Pacific and Rossby wave propagation, *Mon. Weather Rev.*, *127*, 2233–2247.

Ringer, M. A., et al. (2006), The physical properties of the atmosphere in the New Hadley Centre Global Environmental Model (HadGEM1). Part II: Aspects of variability and regional climate, *J. Clim.*, *19*, 1302–1326.

Santos, J., J. G. Pinto, and U. Ulbrich (2009), On the development of strong ridge episodes over the eastern North Atlantic, *Geophys. Res. Lett.*, *36*, L17804, doi:10.1029/2009GL039086.

Scaife, A. A., and J. R. Knight (2008), Ensemble simulations of the cold European winter of 2005–2006, *Q. J. R. Meteorol. Soc.*, *134*, 1647–1659.

Scott, R. K., and L. M. Polvani (2004), Stratospheric control of upward wave flux near the tropopause, *Geophys. Res. Lett.*, *31*, L02115, doi:10.1029/2003GL017965.

Song, Y., and W. A. Robinson (2004), Dynamical mechanisms for stratospheric influences on the troposphere, *J. Atmos. Sci.*, *61*, 1711–1725.

Taguchi, M. (2008), Is there a statistical connection between stratospheric sudden warming and tropospheric blocking events?, *J. Atmos. Sci.*, *65*, 1442–1454.

Thompson, D. W. J., and J. M. Wallace (2000), Annular modes in the extratropical circulation. Part I: Month-to-month variability, *J. Clim.*, *13*, 1000–1016.

Tibaldi, S., and F. Molteni (1990), On the operational predictability of blocking, *Tellus, Ser. A*, *42*, 343–365.

Trenberth, K. E., and K. C. Mo (1985), Blocking in the Southern Hemisphere, *Mon. Weather Rev.*, *113*, 38–53.

Tyrlis, E., and B. J. Hoskins (2008), Aspects of Northern Hemisphere atmospheric blocking climatology, *J. Atmos. Sci.*, *65*, 1638–1652.

Uppala, S. M., et al. (2005), The ERA-40 re-analysis, *Q. J. R. Meteorol. Soc.*, *131*, 2961–3012.

Vallis, G. K. (2006), *Atmospheric and Oceanic Fluid Dynamics*, Cambridge Univ. Press, New York.

van Loon, H. (1956), Blocking action in the Southern Hemisphere, *Notos*, *5*, 171–177.

van Loon, H., and R. L. Jenne (1972), The zonal harmonic standing waves in the Southern Hemisphere, *J. Geophys. Res.*, *77*, 992–1003.

Woollings, T., and B. Hoskins (2008), Simultaneous Atlantic-Pacific blocking and the Northern Annular Mode, *Q. J. R. Meteorol. Soc.*, *134*, 1635–1646.

Woollings, T. J., B. J. Hoskins, M. Blackburn, and P. Berrisford (2008), A new Rossby wave-breaking interpretation of the North Atlantic Oscillation, *J. Atmos. Sci.*, *65*, 609–626.

A. Charlton-Perez, G. Masato, and T. Woollings, Department of Meteorology, University of Reading, Earley Gate, PO Box 243, Reading RG6 6BB, UK. (t.j.woollings@reading.ac.uk)

S. Ineson, Hadley Centre, Met Office, Exeter EX1 3PB, UK.

A. G. Marshall, Centre for Australian Weather and Climate Research, Hobart, Tas 7001, Australia.